

- Enterprise: Economic Viability of Deep Sea-Bed Mining of Polymetallic Nodules* (LOS/PCN/SCN.2/WP.10, United Nations, New York, 1986); C. T. Hillman and B. B. Gosling, *Mining Deep Ocean Manganese Nodules: Description and Economic Analysis of a Potential Venture* (IC 9015, U.S. Bureau of Mines, Washington, DC, 1985).
36. R. Dick, in *The Economics of Deep-Sea Mining*, J. B. Donges, Ed. (Springer-Verlag, Berlin, 1985), pp. 2–60.
  37. E. W. Merrow, K. E. Phillips, C. W. Myers, *Understanding Cost Growth and Performance Shortfalls in Pioneer Process Plants* (R-2569-DOE, Rand Corp., Santa Monica, CA, 1981).
  38. J. E. Halkyard & Co., in *Draft Environmental Impact Statement, Proposed Polymetallic Sulfide Minerals Lease Offering* (U.S. Minerals Management Service, Reston, VA, 1983), pp. 503–545.
  39. Large companies from the United States, Canada, the United Kingdom, Japan, West Germany, France, Italy, Belgium, and the Netherlands have been involved in these efforts [J. M. Broadus, *J. Mar. Resour. Econ.* **3**, 63 (1986)]. Since the abandonment of some earlier approaches, all the consortia members appear to have converged on the hydraulic lift recovery technology, and a 9-year Japanese R&D program with an \$80-million budget seeks to advance this approach by 1989. Seabed mining exploration and R&D programs by the governments of India, China, South Korea, and the Soviet Union are also under way.
  40. P. Hoagland, *J. Resour. Manage. Technol.* **14**, 211 (1985). That the peak in patents precedes the peak in spending is to be expected, since inventive work leading to the patents took place before the expensive at-sea tests of the resulting systems.
  41. The consortia learned through their field work that (i) areal coverage by the nodules is patchier, (ii) the sea-floor terrain is less uniform and holds more obstacles, and (iii) weather conditions are more of a factor than initially expected.
  42. J. E. Stiglitz and G. F. Mathewson, Eds., *New Developments in the Analysis of Market Structure* (MIT Press, Cambridge, 1986).
  43. R. Rafati, in *The Economics of Deep-Sea Mining*, J. B. Donges, Ed. (Springer-Verlag, Berlin, 1985), pp. 62–112 and 253–335.
  44. Advantages of entry cannot be addressed without some attention to failure. See A. Glazer [*Am. Econ. Rev.* **75**, 473 (1985)] and P. Dasgupta [in (42), p. 519]. An executive in one of the British parent companies explained that his group's objective was not to be the first entrant into seabed mining, but to watch and learn from the likely failure of first entrants. He likened the contest to a "slow-speed bicycle race" in which the winner is the last rider to cross the finish line without falling over.
  45. "Statement by the President on the Exclusive Economic Zone of the United States," accompanying Proclamation No. 5030, *Wkly. Compil. Pres. Doc.* **19** (no. 10), 383 (14 March 1983).
  46. The term "strategic materials" has been used in the United States since at least 1922, but its meaning has changed often and still is not precise. A comprehensive review is provided by L. H. Bullis and J. E. Mielke [*Strategic and Critical Materials* (Westview, Boulder, CO, 1985)].
  47. *Strategic Materials: Technologies to Reduce U.S. Import Vulnerability* (OTA-ITE-248, U.S. Office of Technology Assessment, Washington, DC, 1985). The designation was based on the criteria that quantities "required" for "essential" uses exceed "reasonably secure" supplies and that timely substitution seems unlikely.
  48. I gratefully acknowledge the assistance with data compilation and interpretation by P. Hoagland and A. R. Solow and helpful comments from K. O. Emery, J. Padan, and R. M. Solow. Prepared with funds from the J. N. Pew, Jr., Charitable Trust and the Department of Commerce, NOAA Office of Sea Grant, grant NA84AA-D-00033. Woods Hole Oceanographic Institution contribution 6352.

## Covalent Group IV Atomic Clusters

W. L. BROWN, R. R. FREEMAN, KRISHNAN RAGHAVACHARI, M. SCHLÜTER

Atomic clusters containing from two to several hundred atoms offer the possibility of studying the transition from molecules to crystalline solids. The covalent group IV elements carbon, silicon, and germanium are now being examined with this long-range objective. These elements are particularly interesting because of the very different character of their crystalline solids and because they are intermediate between metals and insulators in the nature of their bonding. Small mass-selected atom cluster ions are formed by pulsed laser techniques and identified by time-of-flight methods. Laser photoexcitation is used to study the relative stability of these clusters and their modes of fragmentation. These modes for  $C_n^+$  clusters,

which tend to fragment with a characteristic loss of a neutral  $C_3$ , are found to be different from the modes for  $Si_n^+$  and  $Ge_n^+$  clusters, which tend to fragment to "magic" clusters such as  $Si_4^+$ ,  $Si_6^+$ , and  $Si_{10}^+$ . These experimental results can be accounted for by recent theoretical calculations of the ground-state structure and stability of small silicon and carbon clusters. Several theoretical approaches give consistent results, showing that small silicon clusters are compact and different from small fragments of the bulk crystal. Calculations show that carbon clusters change from linear structures toward cyclic structures as the cluster size increases, but with significant odd-even differences.

SCIENTIFIC INVESTIGATIONS OF THE PROPERTIES OF CLUSTERS of atoms have expanded rapidly in the last 5 years. The goal in many of these studies is to use clusters with increasing numbers of atoms to understand the transition from molecular behavior to the behavior of bulk condensed matter. The evolution of both the structural arrangement of atoms and the electronic states of the system are of intense interest. In addition, there is a strong technological interest in clusters as unique small systems, for example, as catalysts or for making tailored optical materials.

While there now exists a substantial literature on clusters of rare gas atoms and of metal atoms (1), only recently has attention been focused on clusters of the covalent group IV elements: carbon, silicon, and germanium (2–4). Clusters of these three elements represent intermediate cases between the alkali metal clusters, whose

stability is well described by the free electron model, and the rare gas clusters, whose structure is controlled by simple interatomic pair-potentials. Carbon, silicon, and germanium represent a particularly interesting sequence because of the decreasing importance of  $\pi$ -bonding with increasing atomic number in these covalent systems, while the electronic band structure evolves to a semimetal (graphite) in the case of carbon and to an intrinsic semiconductor for silicon and germanium. Results are also beginning to appear on mixed clusters formed from atoms of group III and V elements (5), GaAs and InP, for example, in which cluster properties depend upon both covalent and ionic bonding. However, this article will discuss only

The authors are with AT&T Bell Laboratories, Murray Hill, NJ 07974.

clusters of the covalent group IV elements and in particular only bare clusters in vacuum, as differentiated from clusters whose external bonds are saturated with other ligands as they typically would be in solution (6). This article will concentrate on the structure and stability of these small clusters.

Before 1984, the only experimental work on silicon clusters was by Honig (7) who formed neutral clusters in an oven above molten silicon and measured their relative abundances up to  $\text{Si}_6$ . Work on carbon clusters had been reported in several early papers (8) and  $\text{C}_2$  and  $\text{C}_3$  are now relatively well-characterized species, but very little is known about larger clusters. In 1984 Tsong (9) used photostimulated desorption in a field-ionization atom probe to produce silicon cluster ions. Also in 1984 Rohlifing *et al.* (2) reported work on larger carbon clusters formed by pulsed laser evaporation and coarsely bracketed their ionization potentials. More recently, also using pulsed laser evaporation, Bloomfield *et al.* (3) and Heath *et al.* (4) reported photofragmentation studies of mass-resolved silicon and germanium cluster ions. Kroto *et al.* (10) reported additional studies on larger carbon cluster ions with emphasis on  $\text{C}_{60}^+$ . Silicon clusters have also been seen in the pyrolysis of silanes (11).

Theoretical work on these systems has consisted mainly of a few ab initio calculations on small clusters (12) ( $\text{Si}_2$ ,  $\text{C}_2$  to  $\text{C}_4$ ) and some semiempirical calculations on larger clusters (13). Recently Pacchioni and Koustecky (14) have reported calculations on equilibrium geometries of small clusters of germanium and silicon. The stability of silicon clusters has also been considered by Phillips (15). Calculations by Raghavachari and Logovinsky (16) and by Tománek and Schlüter (17) concur on the structures of several small neutral silicon clusters, all of which are very different from small pieces of the silicon bulk lattice. Small carbon clusters have also been studied recently by different theoretical techniques (18, 19).

Only the preliminary features of a real understanding of the properties of the group IV clusters are beginning to evolve. For example, there is no experimental indication yet as to the cluster size at which conduction and valence bands develop from isolated electronic states in  $\text{Si}_n$  and  $\text{Ge}_n$  molecules. Nor is it evident at what point the familiar regularity of tetrahedral diamond bonding controls the molecular structure. Experimentally it is not even clear at what cluster size carbon clusters form rings, or three-dimensional shells, rather than linear molecules. But clues are beginning to emerge, strongly complemented by theoretical calculations of the structure of these covalent clusters.

## Experimental Cluster Formation and Fragmentation

The formation of clusters of rare gas and metallic elements has primarily been carried out in a supersonic jet expanding into vacuum from a region at a pressure of hundreds of torr (1). The expanding and cooling gas provides for thousands of collisions of any given atom before the mean free path becomes so long, as the pressure decreases, that collisions effectively cease. During the expansion phase, clusters of atoms may form by nucleation and growth. Only a small fraction of the atoms actually form into clusters; the other atoms are needed to carry away the heat of condensation of the clusters, or they would not be bound.

These techniques work very well for elements whose vapor pressure is adequately high at moderate temperature. Maintaining sufficient purity at very high temperatures is difficult, particularly for studies of clusters of highly reactive species. Smalley and his co-workers (20) have greatly extended the range of elements accessible to cluster formation by using nanosecond pulsed lasers to evaporate the material of interest into a buffer gas (usually helium). Clusters

nucleate and grow in the buffer. The gas mixture then expands and cools as in the steady-state case. The pulsed character of the source lends itself naturally to time-of-flight separation of the clusters. Many research groups are now making use of various modifications of this generic approach (1).

A schematic diagram of the apparatus (21) that we used to study group IV clusters is shown in Fig. 1a. It provides a pulsed source of cluster ions, uses time-of-flight techniques to isolate a given cluster size, and incorporates a second pulsed laser, time-synchronized with the first, to produce photofragmentation. The apparatus is cycled at 10 Hz. Each cycle starts with the production of the cluster ions. A pulsed valve produces a short burst of helium, which flows down a narrow channel over a rotating target rod (silicon, germanium, or carbon). Light from a pulsed Nd:YAG (yttrium-aluminum-garnet) laser is focused onto the rod where it vaporizes a portion of the material, producing a plasma entrained in the helium carrier gas. The cluster ions are formed in the multiple collisions during this entrainment and are cooled as the carrier gas expands through the small orifice of the source into the main vacuum chamber. The expansion results in a narrow velocity distribution centered at a velocity of  $\approx 1.5 \times 10^5$  cm/sec corresponding to a kinetic energy of

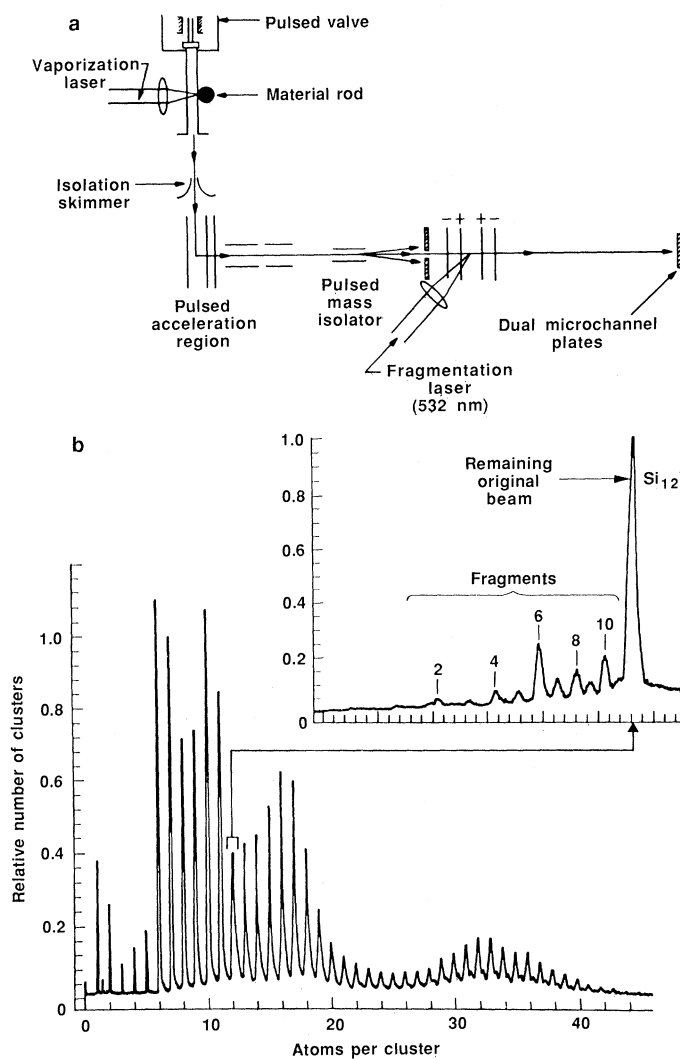


**Fig. 1.** (a) Schematic of the equipment used for photofragmentation studies of covalent group IV atomic clusters (3). The clusters are produced via laser vaporization and separated in a time-of-flight region. (b) A mass spectrum obtained for silicon; the "magic" numbers  $\text{Si}_6^+$  and  $\text{Si}_{10}^+$  are evident. The inset shows the distribution of mass-separated fragments, after  $\text{Si}_{12}^+$  is isolated by the mass isolator and photofragmented.

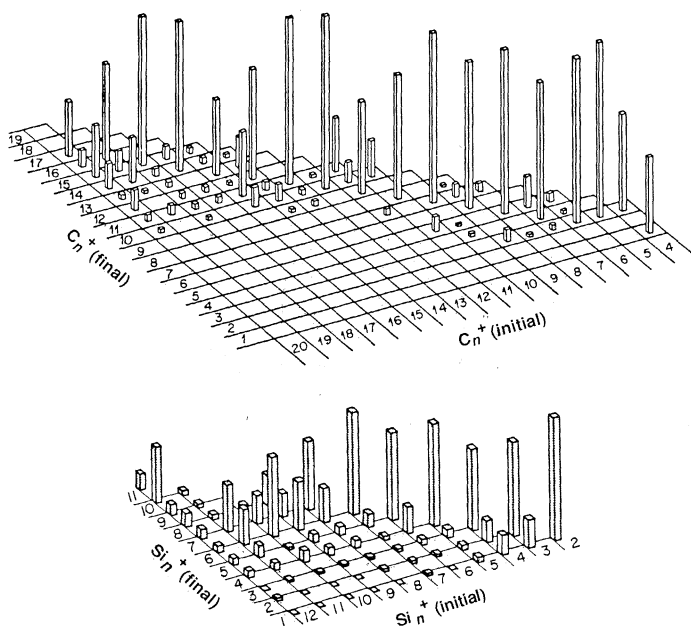


**Fig. 2.** Bar graph of the fragmentation patterns for  $\text{Si}_n^+$  and  $\text{C}_n^+$ . There is a surprising difference between these two cases: for  $\text{Si}_n^+$ , there are magic fragment ions  $\text{Si}_6^+$  and  $\text{Si}_{10}^+$  (shown in the figure only for the smallest parent for which it is dominant); for  $\text{C}_n^+$ , the major fragment is neutral  $\text{C}_3$ , leaving  $\text{C}_{n-3}^+$ .

about 2 eV for a  $\text{Si}_6^+$  cluster. The cluster ion beam then passes through an isolation skimmer into a differentially pumped region where it enters the acceleration grid system. These three grids are pulsed on to coincide with the arrival of the pulse of clusters, and the singly charged cluster ions are all given the same kinetic energy (several kiloelectron volts) in a direction perpendicular to the expansion.

In the first time-of-flight region, the cluster ions separate according to their mass and enter a pulsed mass isolator. This isolator deflects all clusters out of the beam except when it is pulsed off: by adjusting the timing of the control pulse to the isolator, only the clusters having the mass of interest are allowed to proceed.

The mass-selected clusters are then decelerated and exposed to the light from the fragmentation laser, and the resulting charged photofragments are accelerated and dispersed in the second time-of-flight region. The fragments are detected with a dual microchannel electron multiplier. Figure 1b shows the spectrum of  $\text{Si}_n^+$  clusters obtained when the pulsed isolator is not used (3). This spectrum shows the existence of "magic" numbers in the distribution; that is, the relative abundance of a specific cluster is significantly greater than that of its neighbors. The origin of these magic numbers has been the subject of speculation by many investigators (15, 17): is it evidence for unusual stability of these clusters, or does it reflect kinetic hindrances or enhancements in the growth of clusters in the gas expansion?

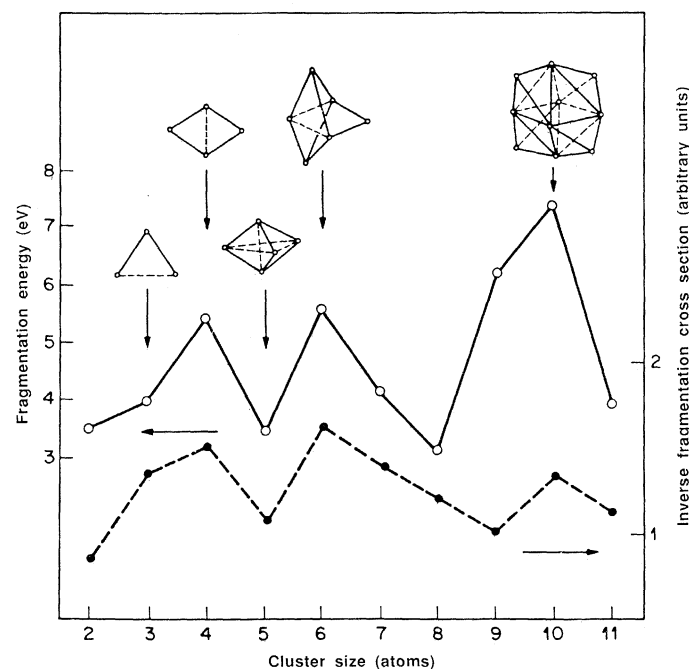
Experimentally it has been found that the cluster distribution often depends on the specific experimental conditions of the measurement (21). However, the mass isolator as shown in Fig. 1a bypasses the question of cluster formation completely. The characteristics of a particular cluster size are investigated independently from the abundance of that cluster in the original spectrum. The inset in Fig. 1b shows what happens when  $\text{Si}_{12}^+$  is isolated from the original spectrum, exposed to a strong photofragmentation laser, and sent with its photoproducts through the second time-of-flight region. This photofragmentation spectrum is decoupled from the conditions of the cluster source and reflects information about the structure or energetics of the  $\text{Si}_{12}^+$  system.

Figure 2 shows the product distribution for photofragmentation (3, 22) of  $\text{Si}_n^+$  and  $\text{C}_n^+$ , depicted as relative probabilities for a cluster of one size to result in an ion fragment of another size. There is a remarkable difference between the two sets of results. The photofragmentation of silicon yields the magic cluster ion  $\text{Si}_6^+$  which is dominant for parent cluster sizes in the range  $n = 7$  to 11. A similar magic fragment,  $\text{Si}_{10}^+$ , is only shown in Fig. 2 for the smallest parent from which it appears, but for a series of larger parents it remains the dominant product. The fragmentation properties of  $\text{Ge}_n^+$  clusters are very similar to those of  $\text{Si}_n^+$  clusters (3, 4), displaying magic photofragmentation species at  $\text{Ge}_6^+$  and  $\text{Ge}_{10}^+$ . In contrast, the photofragmentation spectrum for carbon yields neutral  $\text{C}_3$  as the dominant fragment: larger clusters tend to fragment with the loss of  $\text{C}_3$  leaving a  $\text{C}_{n-3}^+$  ion. We will discuss the implication of these results based on the theoretical structure of  $\text{Si}_n$  and  $\text{C}_n$ .

### Cluster Structure and Stability: Silicon

Until recently there have been very few theoretical efforts to determine the nature of bonding in small silicon clusters (12, 13). In fact, reliable calculations even on the trimer  $\text{Si}_3$  (23) have been available only since 1985. In concert with our experiments, we have carried out theoretical studies to investigate the structural and electronic properties of small silicon clusters (2 to 14 atoms) (16, 17). These studies were based on widely different calculational methods, such as Hartree-Fock plus electron correlation (24), density functional (25), and semiempirical tight-binding (17) theories. In spite of these technical differences, a consistent picture of the structure and bonding in silicon clusters has emerged.

The calculated structures of the small silicon clusters reveal several interesting features. In general, the silicon clusters appear to be completely different from the corresponding carbon clusters. For example,  $\text{Si}_3$  has a bent ground-state geometry whereas  $\text{C}_3$  is



**Fig. 3.** Calculated fragmentation energy for small silicon clusters as a function of cluster size. The fragmentation is defined here as  $\text{Si}_n \rightarrow \text{Si}_{n-1} + \text{Si}$ . The results shown as a solid line are combined results from (16, 17). They are compared to an experimental quantity (dashed curve), the inverse of the fragmentation cross section as given in (3). Also shown are some of the calculated cluster geometries (16, 17).

experimentally known to be a linear molecule (26). Our energy minimization reveals that three-dimensional structures are important for silicon clusters whereas the corresponding carbon clusters are found to be linear or planar (19, 27). Some of our calculated ground-state silicon cluster structures are shown in Fig. 3.

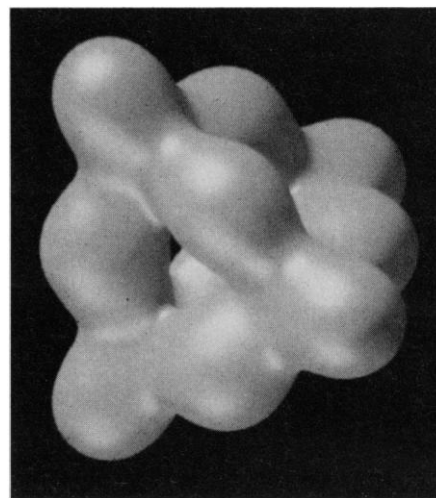
An important question regarding the nature of the calculated cluster geometries is whether these clusters can be considered as small pieces of the bulk crystal. Such microcrystalline structures have been considered for several of the small silicon clusters (3, 9). In particular, a pyramidal structure for Si<sub>4</sub>, a tetrahedral structure for Si<sub>5</sub>, a hexagonal "chair" form for Si<sub>6</sub>, and an "adamantane" type fragment geometry for Si<sub>10</sub> are some of the obvious possibilities derived from the diamond lattice for silicon. One of the principal conclusions from our theoretical studies (16, 17) is that the lowest energy structures are considerably more stable (by  $\approx 0.5$  to 1.0 eV per atom) than the microcrystalline type structures for all these clusters. This is due to the fact that the microcrystalline geometries for these small silicon clusters have, on average, less than 2.5 bonds per atom. The resulting dangling bonds act as a large driving force for additional bond formation leading to considerable structural modifications. However, the energy gained as a result of such bond formation has to be weighed against the strain energy that may be present in the more compact structures. This balance between two opposing factors results in ground-state structures for some of these clusters that may be unexpected. For example, a planar rhombus structure is the ground state of Si<sub>4</sub> and is considerably more stable than a tetrahedron because of the high strain energy present in the latter.

Another important question concerns the possible presence of other low-lying minima on the potential energy surface. If there are a large number of minima with small barriers separating them, then the assignment of unique structures to represent the clusters may not be meaningful. However, with the exception of the smallest clusters, Si<sub>2</sub> and Si<sub>3</sub>, all the calculated silicon structures appear to be fairly well-defined minima without the presence of very low lying isomeric states (16, 17). Moreover, the ground-state geometries of neutral and positively charged silicon clusters are very similar, since the electron that is removed upon ionization comes mainly from a nonbonding orbital. Thus, the calculated ground-state structures can realistically be expected to represent the species observed experimentally.

Inspection of all the calculated minimum energy structures for Si<sub>3</sub> through Si<sub>10</sub> reveals that the nature of the clusters can be understood in a building-block manner (16). Each cluster Si<sub>*n*</sub> can be considered as being built from a smaller cluster Si<sub>*n*-1</sub> by the addition of a silicon atom along an edge (edge cap) or a face (face cap). In the case of the smaller clusters, edge-capped structures appear to be prominent, though face-capped structures are seen in some of the larger clusters. Thus, the planar rhombus structure of Si<sub>4</sub> (Fig. 3) can be considered as an edge-capped triangle, whereas the alternative face-capped form (tetrahedron) is much less stable because of the high strain present. The ground-state structure for Si<sub>5</sub> is three-dimensional and can be formed by bending the rhombus around the short diagonal and by adding another edge-capping atom along this bend to make three equivalent caps. This leads to a compressed trigonal bipyramidal structure for Si<sub>5</sub> (Fig. 3). The structure for Si<sub>6</sub> is an edge-capped trigonal bipyramid, which can also be considered as a distorted octahedron (Fig. 3).

Face-capped structures begin to become important at about Si<sub>6</sub> because of the possibility of additional relaxations which reduce the strain. The ground state of Si<sub>7</sub> can be considered as a face-capped octahedron where there is considerable structural relaxation at that face. Si<sub>8</sub> and Si<sub>9</sub> can be derived from bicapped and tricapped octahedral structures. Si<sub>10</sub> is a tetracapped octahedron where alter-

**Fig. 4.** Computer-generated picture of the Si<sub>10</sub> cluster as defined by a calculated constant-valence charge-density contour. The picture has been generated by D. P. Mitchell, using a ray-tracing algorithm.



nate faces of the octahedron have been capped to yield a highly compact structure with overall tetrahedral symmetry. However, the bonding within the atoms forming the octahedron is fairly weak (2.65 Å) and most of the bonding comes from the cap atoms (2.35 Å, representative of a Si-Si single bond). Thus Si<sub>10</sub> is a loosely bound octahedron held together by the cap atoms. This compact structure, which has almost tetrahedral shape (Fig. 4), is more stable by about 9 eV than the relaxed crystalline adamantane fragment, which we predict to be metastable (17). Similar face-capped structures have been observed on the Si(111) 7 × 7 reconstructed surface (28).

A consideration of the hybridization of the silicon atoms [from a Mulliken population analysis (29)] also helps us understand the nature of the bonding in these clusters. Most of the silicon atoms in the larger clusters have a hybridization of  $\approx s^{1.5}p^{2.5}$ , intermediate between that of a free atom ( $s^2p^2$ ) and that in the bulk ( $sp^3$ ).

As we have seen, the equilibrium structures of small silicon clusters deviate significantly from those of the corresponding crystalline fragments. This is related to the many broken bonds that would exist if the diamond structure were preserved. They act like a surface tension that drives the clusters to more compact structures. A simple estimate of the critical cluster size for the crossover from the dense cluster structures to the open diamond structure can be given. For this, we consider Si<sub>10</sub> as "mostly surface" and compare the energy difference between the open adamantane cage structure and the dense ground-state structure (0.9 eV per atom) (17) with calculated bulk energy differences for diamond-like and close-packed silicon (-0.4 eV per atom) (30). If we now consider a large cluster as composed of both bulk and surface atoms and use the energy differences given above, we can estimate the cluster size for which the total energy difference between open and dense structures goes to zero. This rough estimate predicts the crossover to the bulk structure to occur for clusters of several hundred atoms (17).

What can be said about the relative stability of small silicon clusters and magic numbers? The relative stability of Si<sub>*n*</sub> clusters can be determined if the photofragmentation experiment is interpreted as an equilibrium experiment. Consider the cohesive energy per atom,  $E_{\text{coh}}$ , plotted against cluster size. This is a generally increasing function, rising from 1.6 eV for Si<sub>2</sub> to 4.6 eV for bulk silicon (30, 31). If one assumes, to lowest order, a smooth, monotonic function for  $E_{\text{coh}}$ , one finds that single atom "evaporation" is the energetically most favorable process for fragmentation. This general result holds unless particularly stable structures (magic numbers) occur that dominate the fragmentation channels. The calculations indicate such magic numbers for  $n = 4, 6,$  and 10 (Fig. 3), which is

consistent with the observed fragmentation pattern (Figs. 2 and 3). This consistency is supportive of the interpretation that these experimentally observed fragments are equilibrium clusters, but it does not constitute a proof. The pathway for fragmentation remains a major unanswered question.

## Cluster Structure and Stability: Carbon

Accurate calculations (19) have also been performed on small carbon clusters ( $C_2$  to  $C_{10}$ ). In this case, the behavior is completely different from that of silicon clusters; in carbon, the difference is principally due to the strong  $\pi$ -bonding. This leads to the formation of linear or monocyclic ground-state structures involving multiple bonding. Fused-ring structures more closely related to the graphite fragment, such as the "naphthalene"-like form of  $C_{10}$ , are much less stable as a result of high strain energy.

If the small carbon clusters  $C_n$  are represented as linear structures ( $2n - 2$   $\pi$ -electrons) the odd-numbered clusters may be expected to be stable singlet states and the even-numbered clusters may be expected to be triplet states that are comparatively less stable (27). However, our structural studies (19) indicate that many of the even-numbered clusters prefer to assume monocyclic structures ( $n$   $\pi$ -electrons and  $n$  in-plane pseudo  $\pi$ -electrons for  $C_n$ ) which are more stable (Fig. 5). This is particularly true for  $C_5$  and  $C_{10}$  where the additional bond energy causes the ground states of these clusters to form ring structures. For  $C_4$  and  $C_8$  our calculations indicate that the energetics of the linear and ring structures are comparable, with the ring structures being slightly more stable. In the case of the odd-numbered clusters (up to  $C_9$ ), the linear forms appear to be the ground states. Thus there is an alternation between linear and monocyclic ground-state structures in the case of these small neutral carbon clusters (32). The calculated minimum-energy ring structures of the even-numbered clusters are not regular polygonal forms but have energy stabilization due to lower symmetry in-plane distortions.

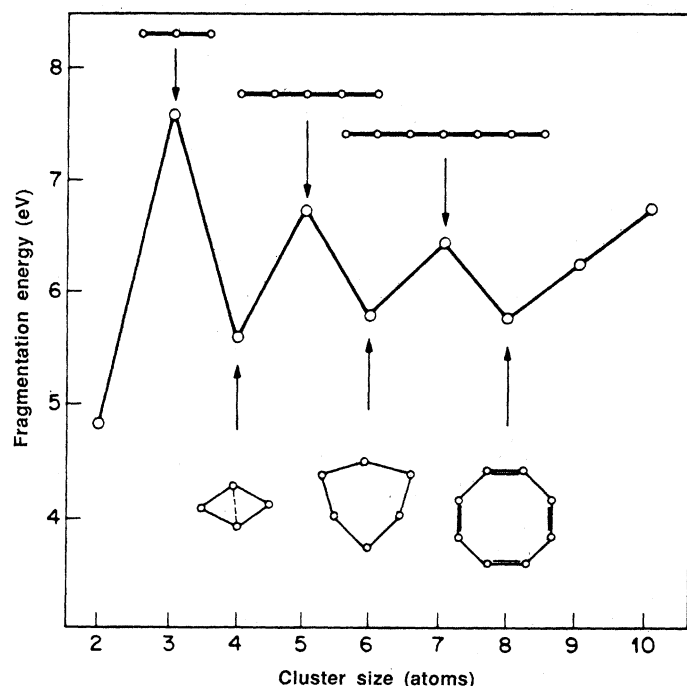


**Fig. 5.** Calculated fragmentation energies of small carbon clusters as a function of cluster size  $n$  for the reaction  $C_n^+ \rightarrow C_{n-1}^+ + C$ . Also shown are some of the calculated cluster geometries for neutral carbon clusters.

As in the case of silicon, it is of interest to speculate on the structures of larger carbon clusters. In a direct comparison between linear and monocyclic structures, we see that as the cluster gets larger ( $>10$  atoms) the cyclic forms will be more stable as a result of the decreasing strain energy. However, much larger clusters will be necessary before the fused-ring, planar, graphite type structures, which have many dangling bonds at the perimeter, become more stable. Recent experimental work by Smalley and co-workers (10) on clusters in the range  $C_{40}$  to  $C_{80}$  is consistent with another alternative, namely, a hollow ellipsoidal or spheroidal shape for these clusters. In particular, these investigators have determined that  $C_{60}$  is a uniquely stable cluster and have proposed a highly symmetric truncated icosahedral structure ("football or soccerball") for this molecule. Such a geometrical arrangement involves no dangling bonds and has been calculated (33) to be very stable with  $\pi$ -electrons delocalized over the entire outer and inner surfaces of the spheroidal structure. However, to our knowledge, no direct experimental evidence confirming such a structure has so far been obtained.

Calculation of the binding energies and ionization potentials of the carbon clusters suggests that odd-numbered clusters up to  $C_7^+$  are more stable than even-numbered clusters. This is consistent with the occurrence of prominent peaks for the odd-numbered  $C_n^+$  in some of the experiments (2, 22). This is also consistent with our experimental determination (34) that  $C_3^+$  and  $C_5^+$  require much more energy for fragmentation than  $C_4^+$ . In contrast to the silicon case, loss of a single atom is not an energetically favorable channel for fragmentation of the small carbon clusters. Our calculations indicate that the lowest energy fragmentation channel for  $C_n^+$  corresponds to loss of neutral  $C_3$ . This is consistent with the experimental observations in Fig. 2. This is partly due to the extra stability associated with the odd-numbered cluster  $C_3$  (Fig. 5). It is also due to the fact that the larger clusters are easier to ionize than the smaller clusters. Thus, if one considers the fragmentation of  $C_{10}^+$ , the channel leading to  $C_7^+$  and  $C_3$  is energetically more favorable than the one leading to  $C_9^+$  and  $C$  because of the extra stability of  $C_3$ . Additionally, it is favored over the channel leading to  $C_5^+$  and  $C_5$  because  $C_7$  has a lower ionization potential than  $C_5$ .

## Outlook

The study of covalent group IV clusters is still in its infancy. Although fundamental issues of growth kinetics and nonequilibrium effects are still unresolved, some important features of the structure and stability of small clusters are well understood. Specifically, it is now possible to account for the major differences that exist between carbon clusters and silicon or germanium clusters. Theoretical calculations of equilibrium cluster structure appear to provide a satisfactory basis for interpreting the experimental measurements of photofragmentation. Studies of the chemical reactivity of clusters are now in progress (35). There are not yet any measurements of the electronic states of small clusters, although photoelectron spectroscopy of mass-selected clusters may soon be feasible. There are also no direct confirmations, by electron or x-ray scattering, for example, of cluster structure. The goal of understanding the transition from molecules to condensed matter requires studies of larger clusters containing dozens or even hundreds of atoms. Such work is just beginning. We expect that the fragmentary picture we now have will be clarified considerably in the next few years.

## REFERENCES AND NOTES

1. O. Echt, K. Sattler, E. Recknagel, *Phys. Rev. Lett.* **47**, 1121 (1981); W. D. Knight *et al.*, *ibid.* **52**, 2141 (1984). For a recent compendium of papers see *Surf. Sci.* **156**, parts 1 and 2 (1985).

2. E. A. Rohlffing, D. M. Cox, A. Kaldor, *J. Chem. Phys.* **81**, 3322 (1984).
3. L. A. Bloomfield, R. R. Freeman, W. L. Brown, *Phys. Rev. Lett.* **54**, 2246 (1985).
4. J. R. Heath *et al.*, *J. Chem. Phys.* **83**, 5520 (1985).
5. S. C. O'Brien *et al.*, *ibid.* **84**, 4074 (1986).
6. R. Rossetti, S. Nakahar, L. E. Brus, *ibid.* **79**, 1086 (1983); L. E. Brus, *ibid.* **80**, 4403 (1984).
7. R. E. Honig, *ibid.* **22**, 1610 (1954).
8. J. Drowart, R. P. Burns, G. DeMaria, M. G. Inghram, *ibid.* **31**, 1131 (1959); D. R. Stull and H. Prophet, *JANAF Thermochemical Tables, National Standard Reference Data Series 37* (National Bureau of Standards, Washington, DC, 1971).
9. T. T. Tsong, *Appl. Phys. Lett.* **45**, 1149 (1984); *Phys. Rev. B* **30**, 4946 (1984).
10. H. W. Kroto, J. R. Heath, S. C. O'Brien, R. F. Curl, R. E. Smalley, *Nature (London)* **318**, 162 (1985); Q. L. Zhang *et al.*, *J. Phys. Chem.* **90**, 525 (1986).
11. T. P. Martin and H. Schaber, *J. Chem. Phys.* **83**, 855 (1985).
12. Some of the leading references are: K. Kirby and B. Liu, *ibid.* **70**, 893 (1979); P. J. Bruna, S. D. Peyerimhoff, R. J. Buenker, *ibid.* **72**, 5437 (1980); R. A. Whiteside, K. Raghavachari, M. J. Frisch, J. A. Pople, P. v. R. Schleyer, *Chem. Phys. Lett.* **80**, 547 (1981); R. A. Whiteside, K. Raghavachari, D. J. DeFrees, J. A. Pople, P. v. R. Schleyer, *ibid.* **78**, 538 (1981).
13. K. S. Pitzer and E. Clementi, *J. Am. Chem. Soc.* **81**, 4477 (1959); R. Hoffmann, *Tetrahedron* **22**, 521 (1966); T. P. Martin and H. Schaber, *Z. Phys. B* **35**, 61 (1979); A. F. Cuthbertson and C. Glidewell, *Inorg. Chim. Acta* **49**, 91 (1981).
14. G. Pacchioni and J. Koutecky, *Ber. Bunsenges. Phys. Chem.* **88**, 242 (1984); *J. Chem. Phys.* **84**, 3301 (1986).
15. J. C. Phillips, *J. Chem. Phys.* **83**, 3330 (1985).
16. K. Raghavachari and V. Logovinsky, *Phys. Rev. Lett.* **55**, 2853 (1985); K. Raghavachari, *J. Chem. Phys.* **84**, 5672 (1986).
17. D. Tománek and M. Schlüter, *Phys. Rev. Lett.* **56**, 1055 (1986).
18. D. W. Ewing and G. V. Pfeiffer, *Chem. Phys. Lett.* **86**, 365 (1982); K. K. Sunil, A. Orendt, K. D. Jordon, *J. Chem. Phys.* **79**, 245 (1984); P. Joyes and M. Leleyter, *J. Phys.* **45**, 1681 (1984); D. H. Magers, R. J. Harrison, R. J. Bartlett, *J. Chem. Phys.* **84**, 3284 (1986); J. Bernholc and J. C. Phillips, *Phys. Rev. B*, in press.
19. K. Raghavachari and J. S. Binkley, *J. Chem. Phys.*, in press.
20. J. B. Hopkins, P. R. Langridge-Smith, M. D. Morse, R. E. Smalley, *ibid.* **78**, 1627 (1983).
21. L. A. Bloomfield, M. E. Geusic, R. R. Freeman, W. L. Brown, *Chem. Phys. Lett.* **121**, 33 (1985).
22. M. E. Geusic *et al.*, *J. Chem. Phys.* **84**, 2421 (1986).
23. K. Raghavachari, *ibid.* **82**, 3520 (1985); G. H. F. Diercksen, N. E. Gruner, J. Oddershede, J. R. Sabin, *Chem. Phys. Lett.* **117**, 29 (1985); R. S. Grev and H. F. Schaefer, *ibid.* **119**, 111 (1985); R. O. Jones, *Phys. Rev. A* **32**, 2589 (1985); K. Balasubramanian, *Chem. Phys. Lett.*, in press.
24. W. J. Hehre, L. Radom, P. v. R. Schleyer, J. A. Pople, *Ab Initio Molecular Orbital Theory* (Wiley, New York, 1986); K. Raghavachari, *J. Chem. Phys.* **82**, 4607 (1985), and references therein.
25. P. Hohenberg and W. Kohn, *Phys. Rev.* **136**, 864 (1964); W. Kohn and L. J. Sham, *ibid.* **140**, A1133 (1965); M. Schlüter and L. J. Sham, *Phys. Today*, **35**, 36 (February 1982).
26. L. Gausset, G. Herzberg, A. Lagerquist, B. Rosen, *Astrophys. J.* **142**, 45 (1965).
27. S. J. Strickler and K. S. Pitzer, in *Molecular Orbitals in Chemistry, Physics and Biology*, B. Pullman and P.-O. Lowdin, Eds. (Academic Press, New York, 1964), p. 281.
28. G. Binnig, H. Rohrer, C. Gerber, E. Weibel, *Phys. Rev. Lett.* **50**, 120 (1983).
29. R. S. Mulliken, *J. Chem. Phys.* **23**, 1833 (1955); *ibid.*, p. 1841; *ibid.*, p. 2338; *ibid.*, p. 2343.
30. M. T. Yin and M. L. Cohen, *Phys. Rev.* **26**, 5668 (1982).
31. K. P. Huber and G. Herzberg, *Constants of Diatomic Molecules* (Van Nostrand, New York, 1979).
32. Ionization to give positively charged carbon clusters can change these results somewhat. Our calculations (19) indicate that the ground state of  $C_{10}^+$  is definitely cyclic but  $C_8^+$  and possibly  $C_6^+$  may be linear.
33. A. D. J. Haymet, *Chem. Phys. Lett.* **122**, 421 (1985); R. C. Haddon, L. E. Brus, K. Raghavachari, *ibid.* **125**, 459 (1986); R. L. Disch and J. M. Schulman, *ibid.*, p. 465; M. D. Newton and R. E. Stanton, *J. Am. Chem. Soc.* **108**, 2469 (1986).
34. M. E. Geusic *et al.*, in preparation.
35. M. L. Mandich *et al.*, *J. Phys. Chem.* **90**, 2315 (1986); *ibid.*, p. 6064.
36. We thank J. S. Binkley and D. Tománek for collaboration on the cluster calculations; L. A. Bloomfield, M. E. Geusic, T. J. McIlrath, and M. F. Jarrold for collaboration on the photofragmentation experiments; and D. P. Mitchell for generating the perspective computer drawing.

## Research Articles

# Immunological Self, Nonself Discrimination

JEAN-GERARD GUILLET, MING-ZONG LAI, THOMAS J. BRINER, SOREN BUUS,  
ALESSANDRO SETTE, HOWARD M. GREY, JOHN A. SMITH, MALCOLM L. GEFTER\*

The ability of immunodominant peptides derived from several antigen systems to compete with each other for T cell activation was studied. Only peptides restricted by a given transplantation antigen are mutually competitive. There is a correlation between haplotype restriction, ability to bind to the appropriate transplantation antigen, and ability to inhibit activation of other T cells restricted by the same transplantation antigen. An exception was noted in that a peptide derived from an antigen, bacteriophage lambda cI repressor, binds to the I-E<sup>d</sup> molecule in a specific way, yet is not I-E<sup>d</sup>-restricted. Comparison of the sequence of the repressor peptide with that of other peptides able to bind to (and be restricted by) I-E<sup>d</sup> and a polymorphic region of the I-E<sup>d</sup> molecule itself revealed a significant degree of homology. Thus, peptides restricted by a given class II molecule appear to be homologous to a portion of the class II molecule itself. The repressor-derived peptide is identical at several polymorphic residues at this site, and this may account for the failure of I-E<sup>d</sup> to act as a restriction element. Comparison of antigenic peptide sequences with transplantation antigen sequences suggests a model that provides a basis for explaining self, nonself discrimination as well as alloreactivity.

IN DIVERSE ANTIGENIC SYSTEMS, IMMUNOLOGICAL RECOGNITION of foreign proteins by T helper cells is directed to a limited number of sites within these antigens (1-4). The T cell recognition sites have been mapped by substituting protein fragments or synthetic peptides for the native antigen in a system in which T helper cell activation in vitro is measured in the presence of antigen-presenting cells. Our findings (5) and those of Babbitt *et al.* (6, 7) showed direct binding of these immunodominant peptides to class II transplantation antigens (present normally on the surface of antigen-presenting cells); these results suggest that at least one role for the class II molecule in T cell activation is to hold the peptide in a favorable conformation for recognition. In addition, these studies demonstrated that the absence of binding of a peptide to the class II molecule can be correlated with immune unresponsiveness for certain antigen-strain combinations. The binding of an immunodominant peptide to a class II molecule is a necessary, but not sufficient, condition to promote immunity. The absence of T cells

J.-G. Guillet, M.-Z. Lai, T. J. Briner, and M. L. Gefter are in the Department of Biology, Massachusetts Institute of Technology, Cambridge, MA 02139. S. Buus, A. Sette, and H. M. Grey are in the Division of Basic Immunology, National Jewish Center for Immunology and Respiratory Medicine, Denver, CO 80206. J. A. Smith is in the Departments of Molecular Biology and Pathology, Massachusetts General Hospital, and the Department of Pathology, Harvard Medical School, Boston, MA 02114.

\*To whom requests for reprints should be addressed.